Meeting the Spatial Needs of the Third Coast

Melanie Gringas[1] and Dr. Michael J. Starek[2]

1. Research Specialist, Texas A&M University-Corpus Christi
2. Associate Professor of Geospatial Systems Engineering, Texas A&M University-Corpus Christi

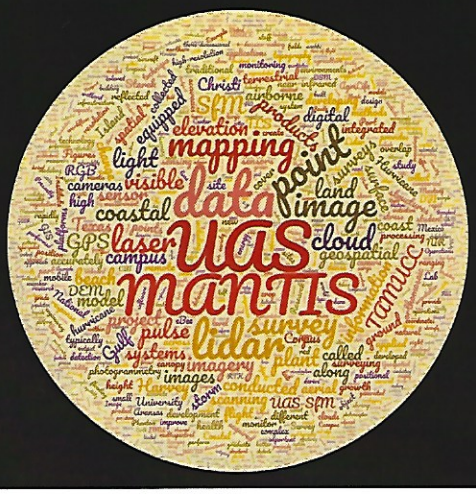

INTRODUCTION

Coastal zones are some of the most dynamic environments on Earth, and some of the most threatened. This reality is likely still on the minds of most residents here in the Coastal Bend after the impacts of Hurricane Harvey last year. According to the United Nations Atlas of the Oceans, more than half of the world's population lives within 200 km of the coast. Growing population demands, threats from storms, and sea encroachment puts coastal communities at the forefront of engineering and scientific efforts. Technically speaking, coastal resilience is a measure of the extent that a coast is able to respond to external pressures without losing actual or potential functions. Improving coastal resilience is considered to be a cost-effective approach to prepare for increasingly uncertain coastal environments. The ability to rebound more quickly can reduce negative impacts to human health, the environment, and the economy. Communities rely on adequate **geospatial data** to guide spatial decision-making in the event of a disaster and for sustainable development and growth. Recent advancements in sensors and platforms for the acquisition of spatially referenced data are rapidly transforming science, society, and decision-making. This revolution is being propelled by emerging technologies such as unmanned aircraft systems (UAS), more commonly referred to as drones, and light detection and ranging (lidar). Such technologies enable us to rapidly map and monitor our evolving world, with unprecedented detail, to tackle a range of problems.

Geospatial data- information that has a geographic aspect to it and represents positions on Earth's surface, including coordinates, an address, or city. There are two basic types of geospatial data: 1) vector-uses points, lines, and polygons to represent spatial features such as cities, roads, and streams; and, 2) raster-uses cells in the form of dots or pixels to represent spatial features. Cities may be a single pixel, roads may be a linear sequence of pixels, and streams are a collection of adjacent pixels.

The Measurement Analytics Lab (MANTIS) of the Conrad Blucher Institute (CBI) for Surveying and Science at Texas A&M University-Corpus Christi (TAMU-CC) explores the merging of **geomatics**, **remote sensing**, and **geospatial computing** to aid scientific and engineering decision-making through improved measurement and analytics of natural and built systems. MANTIS is headed by Dr. Michael Starek, Associate Professor of Civil and Geospatial Engineering. MANTIS gets its name from not only "Measurement" and "ANalyTIcS", but is inspired by the mantis shrimp, which has one of the most impressive multispectral vision systems in nature. The mantis shrimp has upwards of

Geomatics- a branch of science and engineering that deals with the gathering, storing, processing, and interpretation of geographic or spatially referenced data.

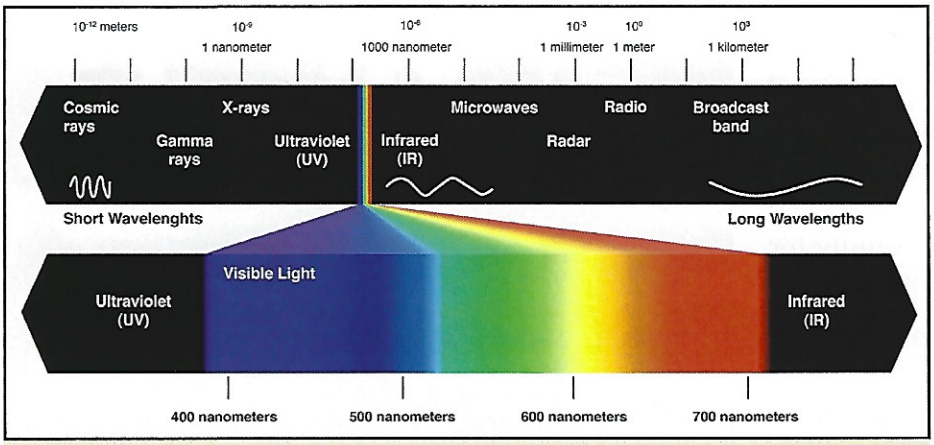

Figure 1: Electromagnetic spectrum (top) with the light that is visible to humans expanded (bottom). Image taken from Iris Tech.

RGB- Red, Green, and Blue; refers to wavelengths of visible light in the red, green and blue part of the spectrum used on a computer display or recorded by a typical digital camera. Red, green, and blue can be combined in various proportions to obtain different colors in the visible spectrum

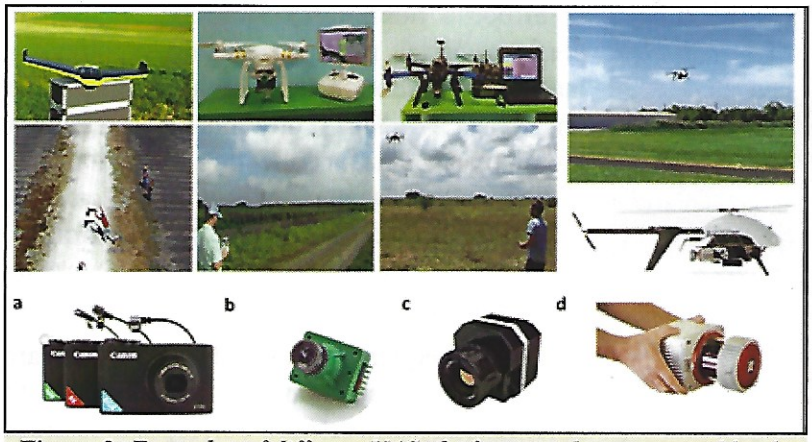

Figure 2: *Examples of different UAS platforms and sensors used by the MANTIS lab at TAMU-CC. (a) Fixed-wing commercial grade mapping system called the SenseFly eBee that comes with a suite of consumer grade cameras modified for visible and near-infrared wavelength capture. (b) DJI Phantom 3 equipped with a 4k* ***RGB*** *camera that and a Sentera near-infrared sensor for agriculture. (c) FLIR VUE Pro thermal sensor integrated on a 3DR X8+ rotary craft. (d) Vapor 55 single-rotary UAS integrated with a survey-grade, high accuracy lidar scanner called the RIEGL VUX-LR (the sensor has a 1350 m effective scanning range). Camera images from the bottom of the collage were taken from the Sensefly, DJI, FLIR, and Vapor manufacturer websites.*

12 or more light-receiving (photoreceptor) cells in its eyes and can detect near-infrared, visible, and ultra-violet spectra of light or twelve-band vision like an advanced satellite multispectral sensor (Figure 1). Humans, on the other hand, are limited to 3 photoreceptor cells for red, green, and blue visible light or three-band RGB (red/green/blue) vision. Unlike the mantis shrimp, the MANTIS Lab uses a fleet of commercial and modified UAS equipped with different types of digital sensors, cameras equipped for mapping and measuring distances (**photogrammetry**), and an array of lidar scanners to extend our ability to monitor and study our surrounding world (Figure 2). This article provides a brief overview on UAS and lidar mapping technology followed by example applications being conducted by MANTIS researchers in the areas of agriculture, facilities surveying, and coastal problem domains.

Remote sensing- scanning and imaging of the earth by satellite, aircraft, or terrestrial platforms in order to obtain information about it.

BACKGROUND

Lidar - Light detection and ranging has become common as a high-resolution and high-accuracy surveying approach for mapping topography and 3D scanning of built and natural structures. Lidar sensors consist of a laser transmitter that sends an outgoing laser pulse and a receiver to collect energy reflected from the surface that is illuminated by the outgoing pulse. The lasers utilized typically operate in the near-infrared (NIR) portion of the electromagnetic spectrum. There are two broad categories applied for ranging: time-of-flight (ToF) and phased-based methods. Pulsed time-of-flight is the most widely applied method for ranging due to the ability to scan at longer distances. By precisely measuring the round-trip time of travel of an emitted laser pulse from the laser transmitter to the object and back and knowing the speed of light, the range (distance) from the lidar sensor to the object can be accurately determined. Lidar systems include a scanning mechanism, such as an oscillating mirror, to direct the laser pulse. Such systems typically pulse the laser at several hundreds of thousands of pulses per second (referred to as pulse repetition rate). This high pulse rate enables very dense sampling of the reflecting surface. Lidar instruments can be operated from the ground on a static tripod (terrestrial laser scanning, TLS) (see Figure 3 below and Figure 9), mobile vehicles (mobile laser scanning, MLS), and in the air (airborne laser scanning, ALS). Spatial referencing of the reflected laser pulse is performed by integrating a global positioning system receiver (GPS) with an inertial measurement unit (IMU) onboard the platform to determine the precise position and orientation of the sensor at the time of each laser pulse (Figure 4a). The main data product output from a lidar survey is a set of densely spaced coordinates providing a three-dimensional representation of the ground and land cover. Collectively, these data points are referred to as a 3D point cloud (Figure 4b). These data can be used to create a digital elevation model (DEM) of topography (bare-earth), digital surface model (DSM) of land cover and built structures (e.g. forests and buildings) and applied for many types of applications such as measuring coastal erosion along a beach or for civil engineering design.

Geospatial computing- the use of computers and specialized software to analyze geographic and spatially referenced data to solve complex problems about the Earth's dynamic systems including natural and human processes.

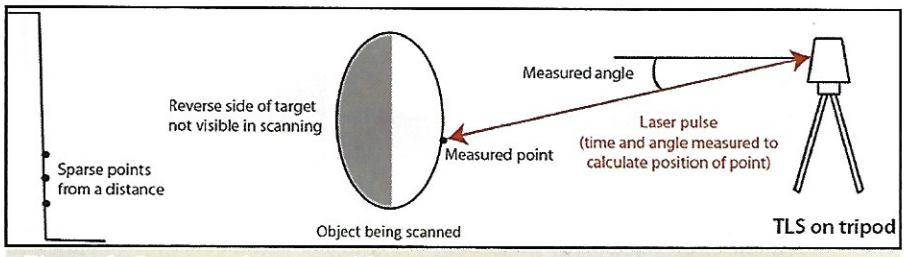

Figure 3: *Process of terrestrial laser scanning to three-dimensionally map structures and objects in the imaged scene.*

Continued on next page

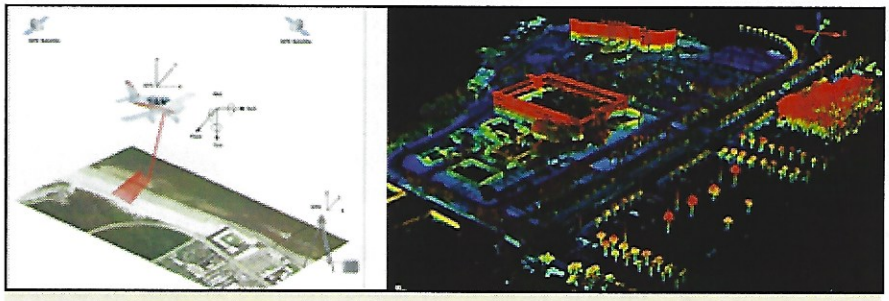

Figure 4: *(a) Example of how airborne lidar works by pulsing a laser and using an oscillating mirror to direct the laser pulse and scan the ground. The GPS and inertial measurement unit (IMU) are used to accurately geolocate the illumination footprint of each laser pulse on the ground. Image from Starek et al., 2012. (b) Example of a 3D point cloud color coded by height generated from a mobile lidar survey of the TAMU-CC campus in 2017. This image shows a portion of the campus including the Conrad Blucher Institute, Carlos Truan Natural Resources Center, and the Harte Research Institute.*

UAS

Small unmanned aircraft systems (sUAS or simply UAS) equipped with miniaturized cameras and sensors provide a new paradigm for aerial surveying and mapping. UAS are used to collect imagery, which can be turned into geospatial data to enable mapping. These data products can be used to characterize developed and natural environments at a level of spatial detail previously unattainable or not practical with traditional remote sensing techniques. Compared to traditional aircraft or satellite remote sensing, UAS provides certain advantages: rapid deploy capabilities, temporal flexibility, cost effectiveness, and high spatial resolution image capture (sub-cm).

Photogrammetry- is the science of making measurements from photographs, especially for recovering the exact positions of surface points.

Photogrammetry is the science of making measurements of objects from photographs, specifically to derive the exact position of a surface point. Input to photogrammetry are image sequences, and common outputs include seamless image mosaics that have been corrected for distortion to allow accurate mapping and 3D models of real-world objects or scenes. Traditional airborne photogrammetry utilizes large-format metric cameras precisely calibrated such that their interior properties, like focal length, are accurately known. However, metric cameras are expensive and not conducive for widespread use of small UAS for mapping applications. In contrast, UAS mapping is typically performed with low-cost consumer grade digital cameras using an emergent technique called Structure-from-Motion (SfM) photogrammetry. SfM exploits information from multiple overlapping images to extract 3D object information (i.e. create point clouds) and negate the need for precise camera calibration. Similar to airborne lidar, UAS-SfM can be used to perform aerial mapping of topography and landcover. Although each technique has pros and cons, UAS-SfM represents a powerful new alternative to lidar for collecting geospatial data. Dependent on the number and size of images, SfM photogrammetry can be computationally intensive. The main stages of SfM processing are summarized below:

1. Image sequences are input into the software and a feature detection algorithm is used to automatically extract and correspond features (called keypoints) between overlapping images.
2. A technique called a bundle block adjustment is then performed to minimize the errors in the correspondences by simultaneously solving for the camera's position and orientation at the time of each photograph. Based on this reconstruction, the matching points are verified and their 3D coordinates calculated to generate what is termed a "sparse point cloud".
3. Finally, the interior and exterior orientation for each image are used with a technique called multi-view stereo-photogrammetry to densify the point cloud by projecting every image pixel onto the surface.

The base data product output from UAS-SfM image processing is a densified 3D point cloud of the scene colored by the RGB values of the camera. UAS-SfM point clouds can be considered hyperspatial (densely-spaced points exceeding 1000 pts/m2) due to the high camera resolution (e.g. 20 MP+) and typical low altitudes at which data are collected. The 3D point cloud can then be used to create a DEM of the terrain, which can subsequently be used to produce a single seamless image, or orthomosaic, from the image sequence. Hence, the geospatial data products output from a UAS-SfM survey are a 3D point cloud, DEM, and orthomosaic. Several commercial and open-source SfM

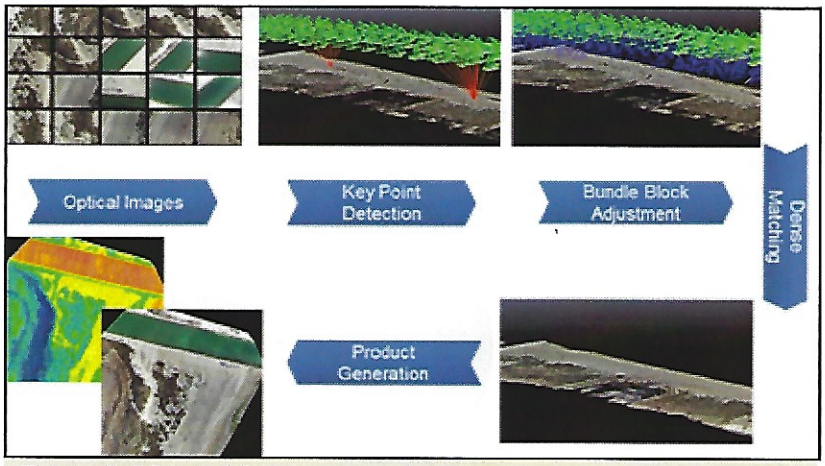

Figure 5: *SfM workflow to process UAS image sequences into densified 3D point cloud, DSM, and orthomosaic. Example here is from Packery Channel.*

software options are available to process UAS imagery. Figure 5 summarizes the UAS-SfM processing workflow.

Aerial SfM can be accomplished with a low-cost hobbyist drone such as the popular DJI Phantom series equipped with consumer-grade digital cameras, or a more expensive commercial-grade survey drone such as the SenseFly eBee series (Figure 2). UAS are integrated with onboard GPS receivers that can be used to overlay the spatial data at their true position on earth (georeferencing). However, the quality of GPS receivers onboard these platforms can highly vary. Most current UAS come equipped with low-accuracy GPS receivers that provide 3D positional accuracies on the order of several to tens of meters whereas some systems come equipped with Real-Time Kinematic (RTK) GPS. RTK GPS is capable of delivering horizontal and vertical positional accuracies down to a few centimeters or less. To improve positional accuracies, ground control targets can be uniformly distributed throughout the study site and their positional coordinates accurately surveyed using a traditional land surveying approach, such as RTK-GPS. These **ground control points** can then be input into the SfM processing workflow (see Figure 5) to more accurately locate the derived geospatial data products on our known longitude and latitude coordinate systems. If done well, UAS-derived image and point cloud products can be accurate to a few centimeters or less from their true positions on the Earth.

To successfully perform UAS mapping, proper flight design is critical. The most important component to consider is image overlap. Significant overlap is essential for the SfM post-processing software algorithms to successfully perform feature matching and reconstruct a three-dimensional model of the imaged surface. In a typical scenario, images are acquired with at least 75% "endlap" (overlap from successive images along the flight line) and at least 60% "sidelap" (overlap between images along adjacent flight lines). For most scenarios, it is recommended that images are acquired with a regular grid pattern. Over more complex environments, more overlap and different flight patterns may be necessary to achieved desired mapping results.

Ground control points- Identifiable targets placed on the ground throughout an area of interest whose coordinates have been precisely surveyed. These targets assist mapping software with accurately positioning aerial imagery in relation to the real world features around it. This process helps to ensure that any point measured on an image map corresponds with its true coordinate location on the ground.

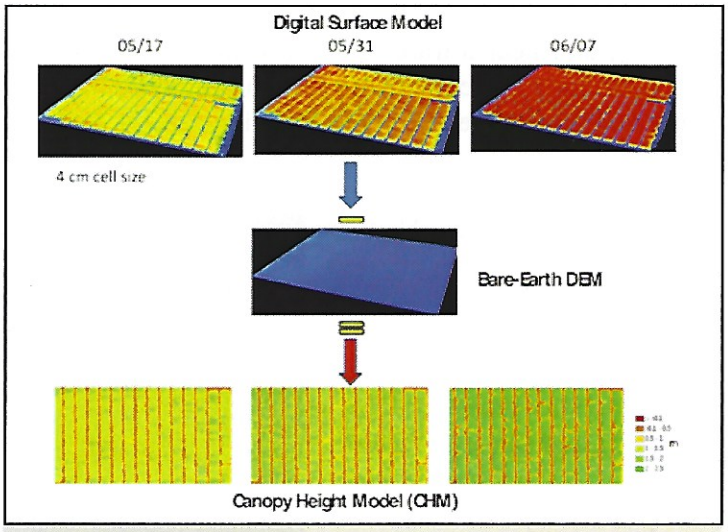

Figure 6: *Examples of UAS-derived canopy height models of cotton and sorghum fields for different survey dates during the summer of 2017 at Corpus Christi AgriLife. 3D point cloud data are used to derive digital surface models (DSMs) of the canopy. A bare-earth digital elevation model (DEM) captured before plant growth is then subtracted from the DSM to compute the canopy height at each grid cell. The result is a raster-based canopy height model which can be used to determine growth rates and biomass*

APPLICATION EXAMPLES

Agriculture - At the Texas A&M AgriLife Research and Extension Center in Corpus Christi (AgriLife), MANTIS graduate students Isabel Garcia and Kevin Wilson conduct UAS surveys of experimental cotton and sorghum fields over the summer growing seasons on a weekly basis. This work has been ongoing since 2014, with the objective of exploring how UAS can be used to better monitor plant health and crop development. Flights at AgriLife are conducted using a variety of platforms including the 3DR Solo and DJI Phantom 4 Pro UAS (see Figure 2) equipped with high-resolution RGB digital cameras. Data from these platforms are used to derive dense 3D point clouds of crop structures to model their structure and canopy growth (e.g. Figure 6). For monitoring crop stress, an eBee SQ platform equipped with a Parrot Sequoia multispectral sensor is flown to collect reflected EM energy across four distinct bands: green visible light (530-

Continued on next page

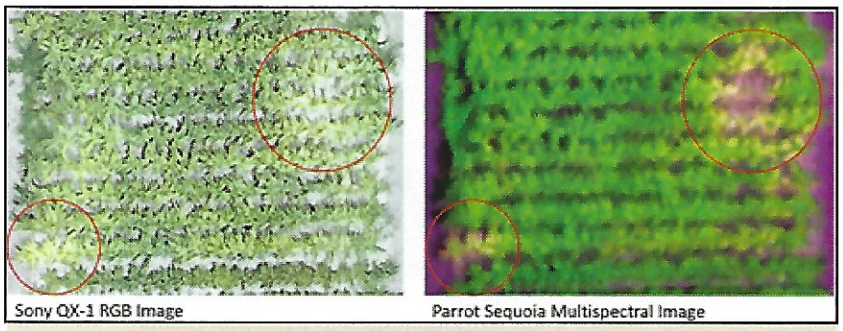

Figure 7: *Comparison of iron chlorosis plant stress visible in high-resolution UAS imagery (left) and visible in falsely-colored red-edge and NIR UAS imagery capturing reflectance patterns not detectable to the human eye (right).*

570 nm), red visible light (640-680 nm), red-edge (730-740 nm), and near-infrared (770-810 nm). Green visible light is strongly correlated with leaf chlorophyll content in plants and more reflected green light indicates a healthier plant. Red visible light is absorbed by healthy vegetation, but reflected more strongly by unhealthy vegetation. Neither red edge nor near infrared (NIR) energy is visible to the naked eye. The reflectance of red edge energy indicates plant stress, such as **iron chlorosis** (Figure 7), and can alert farmers to plant stress before the plant visibly exhibits stress-induced discoloration. NIR is typically used to determine plant vigor and crop type. Results from past studies have shown that UAS can be used to routinely monitor plant health, type, biomass, and growth rates at the "individual plant" level across a single field or entire farm complex much more rapidly and effectively than traditional, antiquated field-surveying approaches.

Iron chlorosis- a yellowing of plant leaves caused by an iron deficiency. In extreme cases, the entire leaf may turn yellow or white and the outer edges will turn brown as the plant cells die.

Facilities Surveying - At TAMU-CC, MANTIS graduate student and Corpus Christi native, Daniel G. Martinez, spearheads the Campus Survey project under the direction of Dr. Starek. The Campus Survey project is supported by the Operations department at TAMU-CC and consists of various survey and geographic information systems (GIS) deliverables that are requested for both the main Ward Island campus and the more recent Momentum campus. These products consist of UAS aerial imagery, topographic land surveys, GIS data products extracted from the UAS imagery, and utility surveying to name a few. By the request of Dr. John Dawson, the Associate Vice President for Operations at TAMU-CC, a new revitalized partnership has begun and is taking shape with the University's first total campus GIS mapping project. The mission of the Campus Survey project is to incorporate the latest in geospatial technology including UAS to assist the Operations department of TAMU-CC. UAS aerial surveys of both Ward Island and Momentum campus are conducted on a quarterly basis under Federal Aviation Administration (FAA) approval. Derived image products are disseminated to campus stakeholders for visualization and analysis using a WebGIS portal developed by MANTIS. These UAS products are being used for a variety of applications including 3D visualization and building information modeling (Figure 8), deriving land survey products for hazards modeling and campus development, and monitoring of infrastructure health and construction. Presently, Daniel's thesis research is focused on developing automated methods for monitoring and detection of campus roof leaks and flexure beyond design performance using UAS imaging approaches. Ultimately, the aim of this partnership is to create a complete and integrated UAS remote sensing, GIS, and land surveying network that will allow University decision makers, operations managers, and essential personnel access to complex multi-layered spatial information in a quick and easy to understand format.

Figure 8: *3D model of the Carlos Truan Natural Resource Center (NRC) on the TAMU-CC campus derived from a recent 2018 UAS aerial survey. This model is a critical component for developing a complete building information model (BIM) of the NRC.*

Coastal Monitoring - MANTIS has several on-going projects along the Texas coast and across the Third (Gulf) Coast. One interesting project partners with Dr. Jim Gibeaut of the Harte Research Institute (HRI) and the Oil Spill Prevention and Response Team of the Texas General Land Office (TGLO) to evaluate the utility of UAS for improving Gulf beach shoreline cleanup and assessment in response to oil spill events. MANTIS graduate student Jacob Berryhill is conducting research to develop "best practices" protocols for integrating small UAS to provide rapid quantitative data on beach morphodynamics and beached oil distribution during a spill response event. As another example, MANTIS's current largest project in terms of the scope of coverage across the Gulf coast is the Regional Geospatial Modeling initiative supported by NOAA's National Geodetic Survey (NGS). This project is a multi-institutional consortium focused on geospatial modeling and height modernization for the northern Gulf of Mexico. Institutional partners include University of Southern Mississippi (lead), Louisiana State University, and University of Florida. The Regional Geospatial Modeling initiative seeks to enhance the National Spatial Reference System adjacent to the northern coast of the Gulf of Mexico, which provides the largest economic return on investment and which is most exposed to inundation from tropical storm surge. The region's unique low-lying coastal topography shows a high risk of inundation posed by projected sea level rise and land subsidence.

As part of this consortium, MANTIS lab is leading the effort on developing and applying advanced **geodetic** imaging and computational techniques to better monitor surface elevation trends and land cover at existing NOAA National Estuarine Research Reserve (NERR) sites across the northern Gulf of Mexico and within low-lying elevation

Figure 9: *(left) Riegl VZ-400 terrestrial laser scanner operated by MANTIS. Shown here is co-author Melanie Gingras operating the scanner for a beach survey. (right) Dr. Michael Starek is releasing the Sensefly eBee for a coastal wetland flight.*

Figure 10: *Mobile lidar scanning system integrated onto a 4WD vehicle for beach mapping. Shown here is former MANTIS post-doctoral researcher, now faculty, Dr. Tianxing Chu.*

Geodetics/Geodesy- the science of mathematically determining the size and shape of the earth, nature of the earth's gravity field, and how these properties change over time.

zones here regionally. Presently, instrumentation and surveys are taking place in coastal marshes and shorelines, which are particularly sensitive to relative sea level rise. Repeated UAS and terrestrial lidar surveys (Figure 9) are being collected at a variety of study sites identified by stakeholders to establish a detailed baseline for long-term vulnerability monitoring and to reoccupy post-event to quantitatively assess change. CBI staff member Alistair Lorde is responsible for conducting terrestrial lidar and long-occupation static and RTK GPS surveys along the Gulf coast from Apalachicola, Florida to Corpus Christi, Texas. CBI/MANTIS staff member Melanie Gingras (article co-author) is responsible for processing the data and overseeing the development of a web portal called "Gulf3D.org" for publicly sharing and visualizing UAS and lidar data products. UAS flight operations, as part of this project, are supported by a cohort of CBI and MANTIS staff and students who have obtained their Part 107 FAA licensure to conduct small UAS operations. MANTIS has also developed a mobile lidar mapping capability using a lidar sensor called the Velodyne HDL 32E integrated with a GPS and IMU for georeferencing by LiDAR USA, Inc. The sensor can be mounted on a 4WD vehicle for beach mapping (Figure 10). Testing and protocol development was conducted by former MANTIS postdoctoral researcher, Dr. Tianxing Chu, in coordination with Dr. Starek. This system provides a rapid mapping capability for post-hurricane response mapping and routine monitoring of beaches and infrastructure along larger swaths of the Texas coast than would be possible with TLS or small UAS. Dr. Chu is now a faculty member at TAMU-CC and part of MANTIS leadership developing a new program in mobile computing and navigation. Finally, the end product of these surveys is typically very large, dense and complex 3D point cloud data (Figure 11). For such data to be applied, automated intelligence is needed to classify points and imagery into meaningful land cover, such as tidal flat or vegetation. Accordingly, MANTIS PhD student Chuyen Nguyen, is developing unsupervised machine learning methods to accurately characterize marsh 3D point cloud data into representative land cover classes for studying marsh evolution. Similarly, MANTIS PhD student, Mohammad Pashaei, is developing "deep learning" methods for object identification and classification within hyperspatial UAS imagery acquired over wetlands and coastal zones. Below is an abridged impact assessment of Hurricane Harvey using data collected by the MANTIS Lab.

Continued on next page

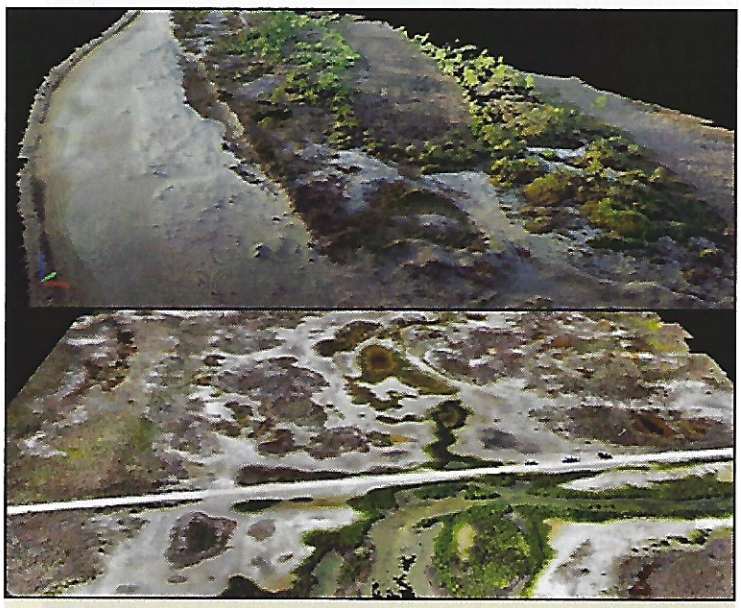

Figure 11: *(top) RGB colored 3D point cloud of Little St. George Island, FL. (bottom) RGB colored 3D point cloud of a wetland study site located on Mustang Island, TX. These point clouds were generated from UAS imagery using structure-from-motion. They are very dense with > 1000 pts/m2. Machine learning methods are being developed to automate intelligent segmentation of points into representative land cover.*

CASE STUDY: HURRICANE HARVEY IMPACT ASSESSMENT

Hurricane Harvey formed as a tropical storm over the Atlantic Ocean on August 17, 2017, weakened to a tropical depression as it crossed the Yucatan Peninsula, but rapidly intensified to a Category 4 strength hurricane in the Gulf of Mexico just before making landfall on the Texas coast 50 km east of Corpus Christi on August 25. Hurricane Harvey caused severe wind damage in coastal towns, extensive flooding as it stalled over Texas from August 25–30, 2017, and unprecedented rainfall with totals in Cedar Bayou reaching 1318 mm (59.89") in just three days.

Shortly after the hurricane, the MANTIS Lab conducted TLS and UAS surveys at various locations along Mustang Island to assess elevation change. Study sites investigated included Gulf-facing beach sites at Port Aransas and Newport Pass and a wetland site on the backside of the island (Figure 12). Change at the beach locations was distinguished by comparing post-hurricane TLS and UAS survey data with pre-storm airborne lidar data collected by the United States Army Corps of Engineers (USACE) National Coastal Mapping Program. The USACE airborne lidar survey was conducted in August-October 2016. The MANTIS lab collected TLS and UAS data in September-October 2017. Figure 13a is a traditional aerial image acquired prior to the hurricane at the Port Aransas South Jetty site, and Figure 13b shows a high resolution UAS orthomosaic image produced from a survey a few weeks after the hurricane. Figure 13c is the airborne lidar DEM created from the USACE survey in 2016, and Figure 13d is the DEM produced from a TLS survey conducted by MANTIS shortly after the hurricane. Figure 13e depicts the differences in elevation following the storm (elevation change) between the airborne lidar and terrestrial lidar DEMs. Results show (Figure 13e) that the most noticeable change was the beach erosion and flooding that took place where as much as 4m (~12ft) was devoured by the large wave action and storm surge experienced in Port Aransas. At Newport Pass, there was perhaps the most noticeable change where a previously weakened dune blowout (Figures 14 a and c) was completely breached by the storm surge during the hurricane and a temporary inlet to Corpus Christi Bay was formed (Figures 14 b and d). This resulted in elevation changes upwards of 4 m (~13 ft) losses where the channel cut through the dune and gains where the flooded bay waters and strong northwest winds from the southern eyewall pushed sediment and water against the backside (bayside) of the dune (Figure 14e). On the bayside, at the Mustang Island Observatory Site (Figures 15a-e), minor, but significant, elevation change was observed when considering the vulnerability of wetlands to subtle elevation change. There were some new channels cut in exposed flats throughout the site and flooding immediately next to the bay was observed. It is important to mention that for this study site, a pre-storm UAS/TLS survey conducted by MANTIS in July 2017 was used to compare with the post-storm UAS/TLS survey.

Figure 12: *Hurricane Harvey Mustang Island study sites of the MANTIS Lab.*

In support of a different initiative related to Harvey, MANTIS lab conducted UAS surveys of heavily damaged neighborhoods in Rockport and Port Aransas as part of a volunteer emergency response effort in collaboration with engineers from the University of Notre Dame and the National Science Foundation (NSF) Geotechnical Extreme Events Reconnaissance (GEER) project. The purpose of the NSF GEER effort is to collect high-resolution remote sensing data along with information on structural damage recorded by reconnaissance teams on the ground to evaluate performance of structures during disaster events. Figures 16a and 16b show aerial images of Rockport, TX prior to Hurricane Harvey and Figures 16c and 16d show parts of a UAS orthomosaic of the same area generated after the storm. Figure 16e is an oblique UAS image of six houses before the storm and Figure 16f is an oblique image of a 3D point cloud constructed from the UAS imagery using SfM. The collected UAS and field data sets from Harvey and other storms are being used by engineers to improve structural design and refine building codes for reducing impacts from hurricanes and other natural disasters.

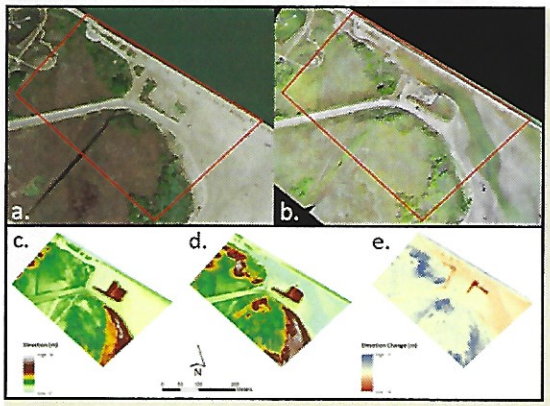

Figure 13: *These images depict storm-related changes to the Port Aransas South Jetty site. (a) Google Earth aerial image from south of the Aransas Pass jetty before Hurricane Harvey; (b) MANTIS UAS imagery from south of the Aransas Pass jetty after Hurricane Harvey; (c) DEM south of the Aransas Pass jetty created from a 2016 USACE airborne lidar survey before Hurricane Harvey; (d) DEM south of the Aransas Pass jetty created from a TLS survey after Hurricane Harvey; (e) Computed elevation change south of the Aransas Pass jetty due to Hurricane Harvey (before DEM surface subtracted from after DEM surface).*

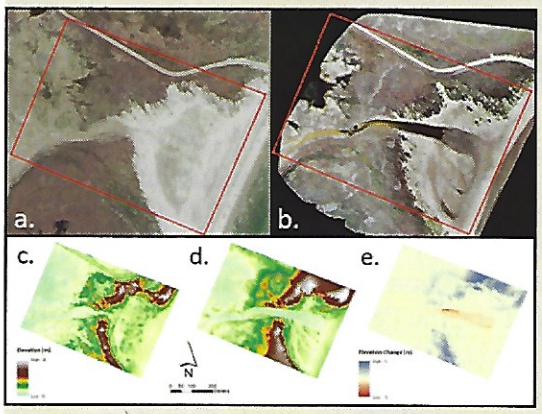

Figure 14: *These images depict storm-related changes to the Newport Pass study site. (a) Aerial image south of Newport Pass before Hurricane Harvey; (b) UAS imagery of Newport Pass after Hurricane Harvey; (c) DEM of Newport Pass created from a 2016 USACE airborne lidar survey before Hurricane Harvey; (d) DEM of Newport Pass created from a TLS survey after Hurricane Harvey; (e) Computed elevation change of Newport Pass due to Hurricane Harvey (before DEM surface subtracted from after DEM surface).*

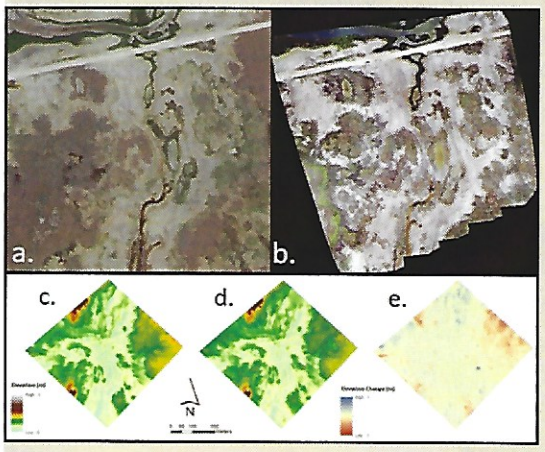

Figure 15: *These images depict the storm-related changes to the Mustang Island Observatory wetland study site. (a) Aerial image of Mustang Island Observatory before Hurricane Harvey; (b) UAS imagery of Mustang Island Observatory after Hurricane Harvey; (c) DEM of Mustang Island Observatory created from a TLS survey conducted approximately two months before Hurricane Harvey; (d) DEM of Mustang Island Observatory created from a TLS survey after Hurricane Harvey; (e) Computed elevation change of Mustang Island Observatory due to Hurricane Harvey (before DEM surface subtracted from after DEM surface).*

Figure 16: *These images depict storm-related changes to a neighborhood near Rockport, Texas: (a) Traditional aerial imagery of a Rockport neighborhood before Hurricane Harvey from Google Earth; (b) Zoomed in view of the aerial image showing the house before Hurricane Harvey; (c) UAS imagery of a Rockport neighborhood after Hurricane Harvey; (d) Zoomed in view of UAS imagery showing damage to the same house after Hurricane Harvey shown in the aerial image above; e) oblique imagery of a Rockport house before Hurricane Harvey; (f) oblique view of a SfM derived 3D point cloud of a Rockport house after Hurricane Harvey.*

As we continue to research and improve the application of UAS and lidar technology, the speed at which we can attain increasingly accurate qualitative and quantitative spatial information skyrockets. Presently, MANTIS uses this information to inform decisions regarding agriculture, infrastructure health, and coastal resiliency but high spatial resolution, three-dimensional data can be applied to and improve a large number of fields. With increasing reliance upon geospatial technology to inform our decisions, it becomes ever more important to understand the accuracies associated with such measurements and how to effectively apply them to better navigate our future world.

For more information about research and developments efforts going on at the MANTIS Lab, please reach out. You can also visit us at our beautiful TAMU-CC island campus; we are located in the NRC 3400 suite.

Dr. Michael Starek, Director,
Michael.Starek@tamucc.edu

Melanie Gingras, Lab Manager,
Melanie.Gingras@tamucc.edu